Materials Science Forum
ISSN: 1662-9752, Vol. 899, pp 148-153
doi:10.4028/www.scientific.net/MSF.899.148

Submitted: 2017-02-14
Accepted: 2017-02-15
Online: 2017-07-03

The Influence of Pr and Mg Content on the Hydrogen Decrepitation of LaNi-Based Battery Alloys

E.P. Soares, L.M.C. Zarpelon and R.N. Faria

Instituto de Pesquisas Energéticas e Nucleares, IPEN-CNEN, São Paulo, Brazil

e-mail:epsoares@ipen.br, zarpelon@ipen.br, rfaria@ipen.br

Keywords: rare earth, transition metal, microanalyses, battery, decrepitation.

Abstract: This paper reports the results of investigations of the hydrogenation and decrepitation of some LaNi-based hydrogen storage cast ingot alloys. A decrepitation procedure for battery negative electrode alloys has been applied using a combination of hydrogen pressure and heating from room temperature to 773K. It has been shown that the Pr and Mg content have a significant influence on the microstructures of the hydrogenated alloys and decrepitation efficiency. Alloys with high concentration of Pr and Mg required an activation quenching treatment for starting the absorption of hydrogen. The decrepitated materials were characterized by scanning electron microscopy (SEM). Electrodes for alloy discharge capacity studies were produced using a nickel screen and electrochemical measurement were carried out in a standard three-electrode cell. The H content of the negative electrode, expressed as the number o H atoms (n) per formula unit, was determined using the measured storage capacity.

Introduction

Ever since the development of $LaNi_5$-based hydrogen storage alloys many investigations have been carried out into the effects of various alloying substitutions made to the basic composition [1-11]. The purpose of the alloy modification is to improve the negative electrode performance of the batteries. It has been reported that, an alloy electrode produced using hydrogen decrepitation was easier to activate than that prepared by mechanical milling [12]. However, no detail of the hydrogen processing of the $La_{0.9}Nd_{0.1}Al_{0.3}Mn_{0.4}Co_{0.75}Ni_{3.55}$ alloy was given in this work. This study addresses this aspect and reports the results of further investigation carried out on the development of a hydrogen decrepitation procedure to substitute mechanical milling of some negative electrode cast ingot alloys represented by the formulae $La_{0.7-x}Pr_xMg_{0.3}Al_{0.3}Mn_{0.4}Co_{0.5}Ni_{3.8}$ and $La_{0.7-y}Pr_{0.3}Mg_yAl_{0.3}Mn_{0.4}Co_{0.5}Ni_{3.8}$ (x=y=0, 0.3, 0.5 and 0.7). The influence of the Pr and Mg content on the decrepitation process has been studied. The hydrogen decrepitated material has been investigated using a scanning electron microscope. Maximum storage capacity of the alloys has also been determined employing a standard electrochemical method for reference. A three-electrode cell with a platinum wire counter electrode and an Hg/HgO reference electrode has been used in this investigation.

Experimental

Commercial alloys in the as-cast state were studied in this work. Ingots were prepared in a rectangular water-cooled copper mould in batches of approximately 5 kg. The chemical compositions of the alloys used in this investigation, a general view of the as-cast alloy microstructures, X-ray diffraction (XRD) patterns and a detailed phase analyses have all been reported in previous papers [13,14]. In order to hydrogenate the cast ingot alloys the following procedure was adopted. Lumps of the alloy (5 g) were cleaned in acetone and manually broken in small pieces (<5 mm). This material was placed in a hydrogenation inconel vessel which was evacuated to backing-pump pressure for 1 hour. Hydrogen was then introduced into the inconel vessel. Hydrogen absorption and decrepitation of the alloys was carried out at room temperature at an initial pressure (P_i) of about 11 bar. Pressure variation was recorded digitally in mbar for improving data precision. Alloys with high Pr (x=0.7) and Mg content (y=0.5 and 0.7) required an

activation quenching treatment from the minimum temperature to start the hydrogen absorption. For decrepitation at lower hydrogen pressure (2 bar) the temperature was raised to 773K and hydrogen absorption started. The decrepitated structures of the specimens were examined using a scanning electron microscope with energy dispersive X-ray analysis facility.

The electrochemical tests for determination of maximum storage capacity alloys were carried out as reported in previous paper [15]. Standard electrodes for determination of alloy maximum storage capacity were prepared by pressing a mixture comprised of 0.1 g of the active powder with carbon black and polytetrafluoroethylene binder, on both sides of a nickel screen. Electrochemical measurements were carried out in a standard three-electrode cell in 6 mol L^{-1} KOH, with a Pt wire counter electrode and an Hg/HgO–KOH/6.0 M KOH reference electrode. Tests were carried out by charging the electrode with a cathodic current of 100 mAg^{-1} for 5 h and discharging with an anodic current of 50 mAg^{-1} to a cutoff cell potential of −600 mV vs. Hg/HgO reference electrode. The hydrogen content of the charged electrode, expressed as the number of H atoms (n) per formula unit, was calculated from the maximum storage capacity (C_{max}) using the Faraday equation [16,17]:

$$n = \frac{3600}{9.65 \times 10^7} Mw \times C\,max$$

where M_w is the molecular weight of the alloy and C_{max} is in units of $mAhg^{-1}$.

Results and discussion

Table 1 gives the hydrogen pressure variation (ΔP) for the Pr-substituted alloys at room temperature (RT) and the number of hydrogen atoms (n) calculated from electrochemically measured C_{max}. A maximum of 2.8 H/f.u. was achieved for the $La_{0.7}Mg_{0.3}Al_{0.3}Mn_{0.4}Co_{0.5}Ni_{3.8}$ alloy. The $Pr_{0.7}Mg_{0.3}Al_{0.3}Mn_{0.4}Co_{0.5}Ni_{3.8}$ alloy exhibited no hydrogen absorption in this processing condition. Figure 1 shows the plots of hydrogen pressure versus absorption time for the alloys with x= 0 and 0.5 processed at room temperature. The hydrogen absorption at room temperature decreases as the amount of Pr on the alloys is increased. Curve profile on hydrogenation is somewhat distinct in each case.

Table 1. Absorption parameters for the Pr-substituted alloys hydrogenated at RT and number of hydrogen atoms per formula unit determined using the electrochemical measured capacity.

x	C [$mAhg^{-1}$]	Mw [$gmol^{-1}$]	n [H/f.u.]	ΔP(RT) [bar]
0.0	192.8	387.1	2.8	3.3
0.3	137.4	387.7	2.0	3.2
0.5	59.3	388.1	0.9	1.8
0.7	45.3	388.6	0.7	0.0

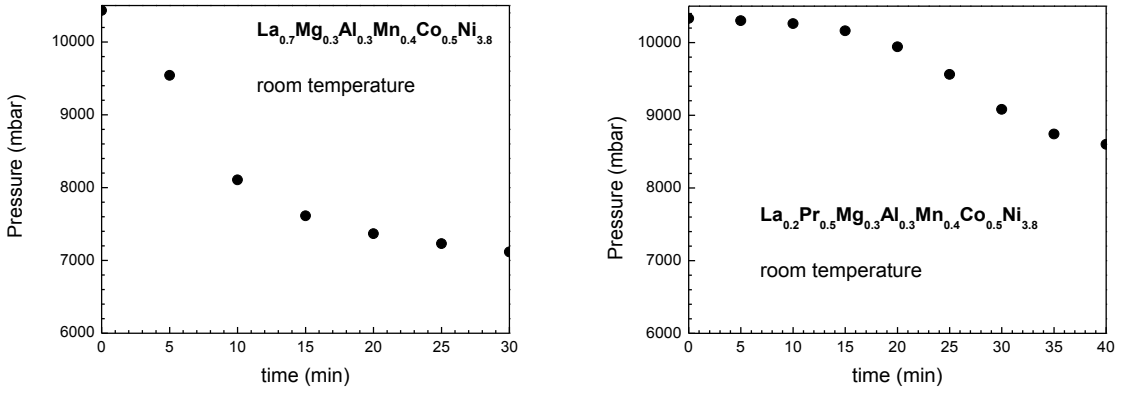

Fig. 1. Pressure versus time for the $La_{0.7-x}Pr_xMg_{0.3}Al_{0.3}Mn_{0.4}Co_{0.5}Ni_{3.8}$ (x=0 and 0.5) alloys hydrogen pulverized at room temperature.

The equivalence between gas and electrochemical absorption has been reported by Cuevas et al. [16]. According to this work, for an alloy absorb a quantity of hydrogen by solid-gas reaction an equivalent electrochemical capacity can be calculated according to the Faraday equation. However, actual electrochemical charge is constrained in open cells by the atmospheric pressure, whereas discharge is limited by corrosion potential of the alloy in conjunction with kinetics and polarizations effects. Hence, reversible electrochemical capacities correspond, at the most, to the hydrogen content loaded by the solid-gas method within the pressure range of about 0.01 to 1 bar. It has also been reported in this work that the $LaNi_5$ alloy is can readily and reversibly absorb 6 H/f.u. at room temperature under an equilibrium pressure of about 2 bar [16]. As observed in the present work, the amount of the additive elements is preponderant on the capacity of LaNi-based alloys to absorb hydrogen.

Table 2 gives the hydrogen pressure variation at room temperature for the Mg-substituted alloys and number of hydrogen atoms calculated from electrochemically measured C_{max}. A maximum of 3.9 H/f.u. was achieved for the $La_{0.7}Pr_{0.3}Al_{0.3}Mn_{0.4}Co_{0.5}Ni_{3.8}$ alloy. Clearly, higher substitutions of La for Mg are not favorable to hydrogen absorption of these negative electrode alloys for nickel-hydride batteries. Thus, the amount of Mg should be kept to a minimum. Figure 2 shows the plots of hydrogen pressure versus absorption time at room temperature for the Mg-substituted alloys. These curves profile show that the hydrogen absorption behavior changes with the introduction of Mg on the alloy. The pressure variation is smaller in the Mg-containing alloy showing inferior hydrogen absorption. The alloys with higher Mg contents (y=0.5 and 0.7) showed no hydrogen absorption in this processing condition.

Table 2. Absorption parameters for the Mg-substituted alloys hydrogenated at room temperature and number of hydrogen atoms per formula unit determined using the measured storage capacity.

y	C [mAhg^{-1}]	Mw [gmol^{-1}]	n [H/f.u.]	ΔP(RT) [bar]
0.0	248.8	422.1	3.9	4.4
0.3	137.4	387.7	2.0	3.5
0.5	35.9	364.8	0.5	0.0
0.7	11.8	341.9	0.2	0.0

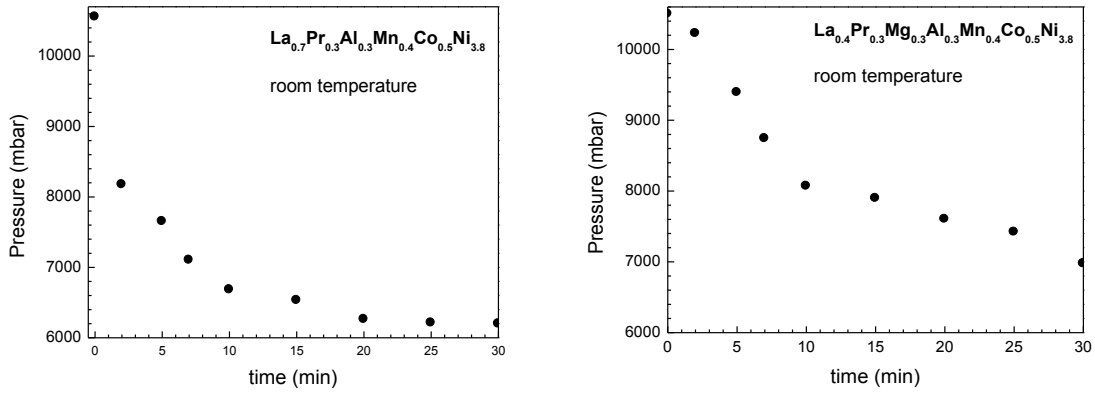

Fig. 2. Pressure versus time for the $La_{0.7-y}Pr_{0.3}Mg_yAl_{0.3}Mn_{0.4}Co_{0.5}Ni_{3.8}$ (y=0 and 0.3) alloys hydrogen pulverized at room temperature.

Figure 3 shows the pressure versus time for the $La_{0.2}Mg_{0.5}Pr_{0.3}Al_{0.3}Mn_{0.4}Co_{0.5}Ni_{3.8}$ (y=0.5) and $Pr_{0.7}Mg_{0.3}Al_{0.3}Mn_{0.4}Co_{0.5}Ni_{3.8}$ (x=0.7) alloys hydrogen pulverized after quenching from 573K. Activation by quenching from 573K was necessary for these alloys to start absorbing hydrogen. The pressure variation was smaller in the alloy without La. An even higher quenching temperature (773K) was necessary for activation of the La-free alloy with larger amount of Mg ($Pr_{0.3}Mg_{0.7}Al_{0.3}Mn_{0.4}Co_{0.5}Ni_{3.8}$ alloy). Total La substitution for Mg (y=0.7) makes the hydrogenation process even more difficult to occur than that of Pr.

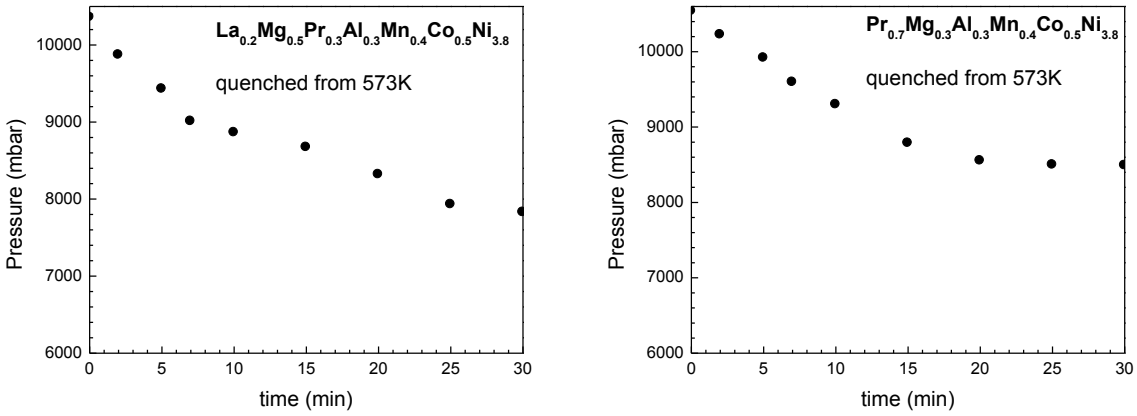

Fig. 3. Pressure versus time for the $La_{0.2}Mg_{0.5}Pr_{0.3}Al_{0.3}Mn_{0.4}Co_{0.5}Ni_{3.8}$ and $Pr_{0.7}Mg_{0.3}Al_{0.3}Mn_{0.4}Co_{0.5}Ni_{3.8}$ alloys hydrogen pulverized at after quenching from 573K.

Figure 4 shows the plots with the variation of the hydrogen pressure versus absorption time at 773K for the $La_{0.7-x}Pr_xMg_{0.3}Al_{0.3}Mn_{0.4}Co_{0.5}Ni_{3.8}$ alloys. In this high temperature all the alloys started spontaneous absorption of hydrogen at a low hydrogen pressure of 2 bar. These curves show that also at this high temperature the absorption of hydrogen decreases somewhat with Pr substitution and changed the absorption curves profile. The alloy without Pr showed the highest hydrogen pressure variation on the absorption time interval of 1 h. Figure 5 shows the SEM microstructures with a general view of the decrepitated material obtained from the cast ingot of the $La_{0.7}Mg_{0.3}Al_{0.3}Mn_{0.4}Co_{0.5}Ni_{3.8}$ and $Pr_{0.7}Mg_{0.3}Al_{0.3}Mn_{0.4}Co_{0.5}Ni_{3.8}$ alloys using the hydrogen treatment at 773K. There was a distinct change in the structure for these powders as the Pr-content was increased. The $La_{0.7}Mg_{0.3}Al_{0.3}Mn_{0.4}Co_{0.5}Ni_{3.8}$ alloy shows clearly a typical hydrogen decrepitation structure. The $Pr_{0.7}Mg_{0.3}Al_{0.3}Mn_{0.4}Co_{0.5}Ni_{3.8}$ alloy absorbed much less hydrogen and showed a microstructure with poor decrepitation features.

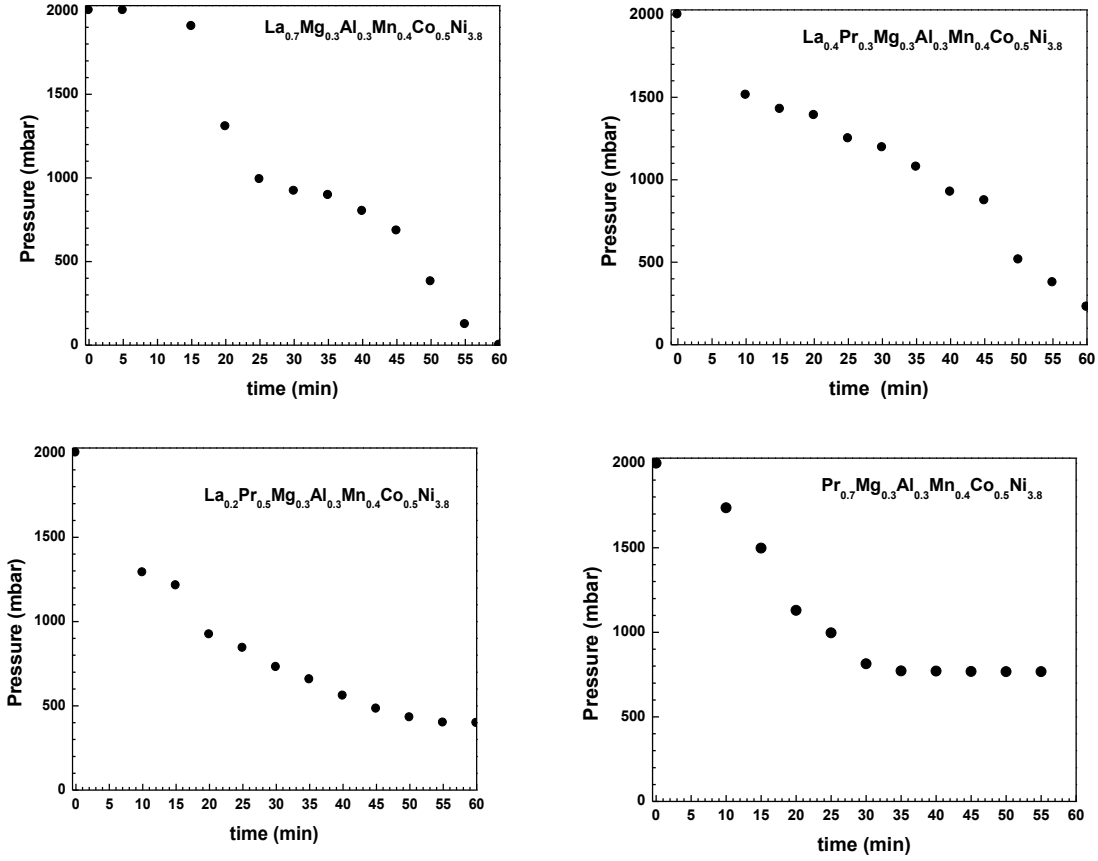

Fig. 4. Pressure versus time for the Pr-substituted alloys pulverized at 773K.

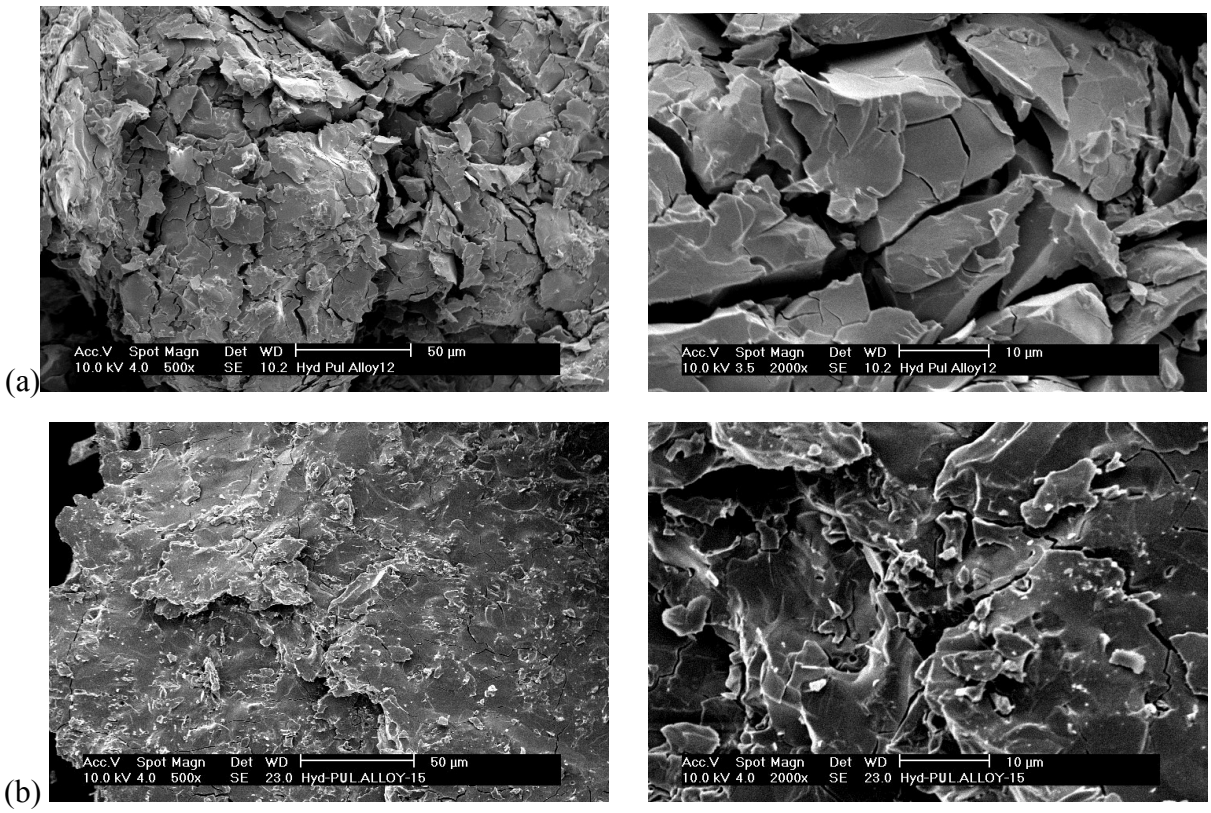

Fig. 5. Backscattered electron images of a general view and details to the microstructures of the pulverized (773K) Pr-substituted alloys; (a) x=0 and (b) x=0.7.

The hydrogenation behavior change on substitution could be partially attributed to the grain structure and phases modifications of these alloys that favor hydrogen absorption. It has been reported that the substitution of La with Pr in the alloys changed the grain structure from equiaxed to columnar [13,14]. In these studies, phase identification using X-ray diffraction and phase analysis showed that the alloys are composed of a matrix phase, a gray phase and a dark phase. The matrix phase revealed a (La,Pr) : (Al,Mn,Co,Ni) atomic ratio of about 5, indicating it to be a 1:5 phase. The gray phase exhibited a concentration of 11 at.% of Mg and EDX ratio of concentration indicated a composition corresponding to RMg_2Ni_9 (R=La,Pr) phase. The proportion of the dark phase, containing Al, Mn and Co, diminished somewhat as the Pr-content was increased in the alloys. All these microstructural and phases changes might also have some influence on the hydrogen hydrogenation behavior observed in this study. Similarly, this also could be the case with structure and phase modification on Mg substitution in these alloys. The electrochemical behavior is in good agreement to the hydrogen absorption characteristics of these alloys. Comparatively, the substitution of La for Mg decreased more significantly the electrochemical capacity of the alloys. The best discharge capacity achieved in these alloys (249 $mAhg^{-1}$) was for the Mg-free alloy ($La_{0.7}Pr_{0.3}Al_{0.3}Mn_{0.4}Co_{0.5}Ni_{3.8}$).

Conclusions

The Pr and Mg content have a significant effect on the hydrogenation/decrepitation process of the LaNi-based hydrogen storage battery alloys. In general, the hydrogen absorption diminished as the amount of these elements in the alloys was increased. The decrepitation process also was less effective in both cases. This has been partially attributed to the changes on the microstructures and phases of the alloys with the Pr and Mg substitutions. Alloys with larger amounts of these two elements required an increased processing temperature or a quenching treatment to activate absorption of hydrogen and the decrepitation process. A maximum of 3.9 H/f.u. has been achieved for the $La_{0.7}Pr_{0.3}Al_{0.3}Mn_{0.4}Co_{0.5}Ni_{3.8}$ alloy. For low substitution contents hydrogen decrepitation was more efficient using high pressure/RT than low pressure/high temperature.

Acknowledgements

The authors wish to thank FAPESP, CNPq and IPEN-CNEN/SP for the financial support and infrastructure made available to carry out this investigation.

References

[1] F. Feng, M. Geng, D.O. Northwood: International Journal of Hydrogen Energy Vol. 26 (7) (2001), p. 725.
[2] A. K. Shukla, S. Venugopalan, B. Hariprakash: Journal of Power Sources Vol. 100 (1-2) (2001), p. 125.
[3] K. Hong: Journal of Alloys and Compounds Vol. 321 (2) (2001), p. 307
[4] R.C. Ambrosio, E.A. Ticianelli: Journal of Power Sources Vol. 110 (1) (2002), p. 73
[5] I.P. Jain, M.I.S. Abu Dakka: International Journal of Hydrogen Energy Vol. 27 (4) (2002), p. 395.
[6] H. Ye, Y.X. Huang, T.S. Huang, H. Zhang: Journal of Alloys and Compounds Vols. 330-332 (2002), p. 866
[7] Y. Liu, H. Pan, M. Gao, Y. Zhu, Y. Lei, Q. Wang: International J. of Hydrogen Energy Vol. 29 (3) (2004), p. 297
[8] H. Pan, Q. Jin, M. Gao, Y. Liu, R. Li, Y. Lei: Journal of Alloys and Compounds Vol. 373 (2004), p. 237.
[9]H. Pan, X. Wu, M. Gao, N. Chen, Y. Yue, Y. Lei: International Journal of Hydrogen Energy Vol. 31 (2006), p. 517.
[10] J. Hongmei, L. Guoxun, Z.Chuanhua, W. Ruikun: Journal of Power Sources Vol. 77 (1999), p. 123.
[11] K. Kadir, D. Noreus, I. Yamashita: Journal Alloys and Compounds Vol. 345 (1-2) (2002), p. 140
[12] H. Pan, N. Chen, M. Gao, R. Li, Y. Lei, Q. Wang: Journal Alloys and Compounds Vol. 397 (1-2) (2005), p. 306.
[13] L.M.C. Zarpelon, E. Galego, H. Takiishi, R.N. Faria: Materials Research Vol. 11 (1) (2008), p. 17.
[14] E.P. Banczek, L.M.C. Zarpelon, R.N. Faria, I. Costa: Journal of Alloys and Compounds Vol. 479 (2009), p. 342.
[15] L.M.C. Zarpelon, R.N. Faria: Materials Science Forum Vol. 802 (2014), p. 421.
[16] F. Cuevas, J.M. Joubert, M. Latroche, A. Percheron-Guegan: Applied Physics A Mat. Sc. and Processing Vol. 72 (2001), p. 225.
[17] J.J. Reilly, G.D. Adzic, J.R. Johnson, T. Vogt, S. Mukerjee, J. McBreen: J. Alloys and Compounds Vol. 293-295 (1999), p. 569.